Anterograde flow of cargo across the Golgi stack potentially mediated via bidirectional ''percolating'' COPI vesicles

Lelio Orci*, Mariella Ravazzola*, Allen Volchuk†, Thomas Engel†‡, Michael Gmachl†§, Mylène Amherdt*, Alain Perrelet*, Thomas H. Söllner†, and James E. Rothman†¶

*Department of Morphology, University of Geneva Medical School, 1 rue Michel Servet, 1211 Geneva 4, Switzerland; and †Cellular Biochemistry and Biophysics Program, Memorial Sloan–Kettering Cancer Center, 1275 York Avenue, Box 251, New York, NY 10021

Contributed by James E. Rothman, June 26, 2000

How do secretory proteins and other cargo targeted to post-Golgi locations traverse the Golgi stack? We report immunoelectron microscopy experiments establishing that a Golgi-restricted SNARE, GOS 28, is present in the same population of COPI vesicles as anterograde cargo marked by vesicular stomatitis virus glycoprotein, but is excluded from the COPI vesicles containing retrograde-targeted cargo (marked by KDEL receptor). We also report that GOS 28 and its partnering t-SNARE heavy chain, syntaxin 5, reside together in every cisterna of the stack. Taken together, these data raise the possibility that the anterograde cargo-laden COPI vesicles, retained locally by means of tethers, are inherently capable of fusing with neighboring cisternae on either side. If so, quanta of exported proteins would transit the stack in GOS 28–COPI vesicles via a bidirectional random walk, entering at the cis face and leaving at the trans face and percolating up and down the stack in between. Percolating vesicles carrying both post-Golgi cargo and Golgi residents up and down the stack would reconcile disparate observations on Golgi transport in cells and in cell-free systems.

The v-SNAREs and t-SNAREs are cytoplasmically oriented membrane proteins that link up between bilayers to form pin-like structures (''SNAREpins'') capable of fusing membranes (1–5). The distribution of cognate v-SNAREs and t-SNAREs among intracellular compartments and their specific patterns of association with each other in cells amount to a virtual roadmap of intracellular vesicle transport pathways (6), and individual SNARE proteins are selectively required for the fusion process *in vivo* at steps corresponding to their locations, suggesting that SNARE pairing provides both the specificity and the driving force for bilayer fusion (2–5). Tethering precedes fusion by SNAREs, increasing the rate of vesicle capture and in the process adding an important layer of spatial and temporal regulation for fusion by effectively restricting SNARE pairing to a defined region of a membrane or organelle (reviewed in refs. 7–9).

The distribution of SNARE proteins within the Golgi therefore has considerable bearing on current debates concerning the pattern and mechanism of protein flow within the stack of cisternae comprising this organelle. While it is known that certain v- and t-SNAREs are required for Golgi function, the precise stage at which they operate and which vesicles, if any, contain them have not been established (10). Yeast has only eight syntaxins (the requisite ''heavy chain'' subunit of t-SNAREs) (5). Only one of these (Sed5p) is essential for function for Golgi transport (11, 12), effectively ruling out the possibility that distinct vesicle shuttles operate at every level of the stack (13). But this genetic evidence does not speak to the possibility that the Golgi may use the same SNAREs over and over again in budding vesicles at every level according to a stochastic mechanism, a possibility to which we address ourselves here. While cisternal progression (13–15) may well be important for transport of certain protein aggregates (15) or Golgi biogenesis, studies to date suggest it is too slow to account for the anterograde flow of most proteins across the stack (16–18).

There is ample evidence of a role for COPI vesicles in anterograde transport across the Golgi stack (19–22), including the fact that a population of COPI-coated vesicles containing anterograde-targeted cargo, but not retrograde-targeted cargo, buds at every level of the stack *in vivo* (23). The fact that COPI vesicles can also mediate retrograde transport from Golgi to the endoplasmic reticulum (ER) (24) confounds the interpretation of standard biochemical or genetic functional tests that might otherwise formally establish the role of COPI vesicles in anterograde flow. Thus, the seemingly remote possibility that the COPI vesicles carrying anterograde-targeted cargo [such as proinsulin or the vesicular stomatitis virus (VSV)-encoded glycoprotein (G protein)] could move *exclusively* in the retrograde direction within the stack (14) could not be rigorously excluded on the basis of current data (23) because of a lack of information in the content of SNAREs in these vesicles.

Materials and Methods

Plasmid Constructions and Cell Lines. The coding sequence of syntaxin 5 was amplified by using a syntaxin 5 cDNA template with primer 1 (AGC TTC CGA ATT CAT GTC CTG CCG GGA TCG GAC CCA GGA G) and primer 2 (CTC AGG CAA GGA AGA CCA CAA AGA TGA T). The PCR product was subcloned into a pTRE vector (CLONTECH), yielding a construct encoding the following amino-terminal amino acid sequence [containing three hemagglutinin (HA) epitopes] MYPYDVPDYAGYPYDVPDYAGSYPYDVPDYALE-SGGKLASEF linked to Syntaxin 5. The sequence was confirmed by DNA sequencing. Stable Tet-Off HeLa cells expressing Syntaxin 5 under transcriptional control were generated according to the manufacturer's instructions (CLONTECH). A cell line expressing similar levels of endogenous and HA-tagged Syntaxin 5 was selected for localization studies.

CHO/F3 cells expressing myc-GOS28 were generated as described in ref. 25.

Antibodies. Anti-Syntaxin 5 antibodies were made by injecting New Zealand White rabbits with a His_6-tagged cytoplasmic

Abbreviations: ER, endoplasmic reticulum; VSV, vesicular stomatitis virus; G protein, glycoprotein.

‡Present address: Institut für Arteriosklerosеforschung, Domagkstrasse 3, 48149 Münster, Germany.

§Present address: University of Vienna Biocenter, Department of Molecular Genetics, Dr. Bohrgasse 9, A-1030 Vienna, Austria.

¶To whom correspondence should be addressed. E-mail: j-rothman@ski.mskcc.org.

The publication costs of this article were defrayed in part by page charge payment. This article must therefore be hereby marked "*advertisement*" in accordance with 18 U.S.C. §1734 solely to indicate this fact.

Article published online before print: *Proc. Natl. Acad. Sci. USA*, 10.1073/pnas.190292497. Article and publication date are at www.pnas.org/cgi/doi/10.1073/pnas.190292497

domain of Syntaxin 5 (His_6-Syntaxin5c), purified from inclusion bodies in the presence of 6 M urea by using a NiNTA–affinity column (Qiagen, Hilden, Germany). Antibodies were affinity purified from serum by affinity chromatography using His_6-Syntaxin5c covalently linked to SulfoLink Coupling Gel (Pierce) according to the manufacturer's protocol. The antibody was used at a 1:20 dilution. The other antibodies used for immunoelectron microscopy were: affinity-purified rabbit anti-GOS 28 (25) (diluted 1:3 and 1:5), anti-KDEL receptor (26) (diluted 1:500), and mouse monoclonal anti-myc 9E10 (diluted 1:20). Anti-VSV G protein antibody (P5D4) was a gift of the late T. E. Kreis (diluted 1:200).

Immunolocalization. For electron microscope immunolabeling, CHO/F3 and HeLa St5/34 cells were fixed with 1% glutaraldehyde in 0.1 M phosphate buffer (pH 7.4), infused with 2.3 M sucrose, frozen in liquid nitrogen, and sectioned with a cryoultramicrotome. Thin sections collected on parlodion-coated grids were immunolabeled as described previously (23). Double immunolabeling for GOS 28 and KDEL receptor was performed on CHO/F3 cells by incubating thin sections with mouse monoclonal anti-myc 9E10 and rabbit anti-KDEL receptor antibodies, followed by anti-mouse and anti-rabbit IgG coupled with gold particles of 10- and 15-nm diameter, respectively. The same procedure was applied for the double immunolabeling of GOS 28 and VSV G protein, using mouse anti-VSV G antibody (10-nm gold particles) and rabbit anti-GOS 28 antibody (15-nm gold particles).

Quantitation of Immunolabeling. The subcellular localization of the different antigens was analyzed quantitatively on thin cryosections. Sections containing Golgi complexes in a suitable cis–trans orientation were photographed and printed at the final magnification of ×96,000. For each antigen, 20 different Golgi areas were quantified. The subcellular compartments evaluated were as follows: (*i*) vesicles in the transitional region (i.e., 70 to 90-nm vesicular profiles present between the cis-most Golgi cisterna and the transitional elements of the rough ER); (*ii*) Golgi cisternae defined as elongated membrane profiles enclosing a lumen; (*iii*) lateral buds and vesicles defined as circular 70 to 90-nm membrane profiles connected (buds) or not connected (vesicles) to Golgi cisternae on the sections. For the evaluation of the cis-to-trans labeling on Golgi cisternae, 20 suitably oriented Golgi complexes were evaluated. The trans pole was identified by the presence of clathrin-coated vesicles. The distribution of gold particles over individual Golgi cisternae (cisterna 1 = cis-most, cisterna 5 = trans-most) was expressed as a percentage of the total number of gold particles present in the

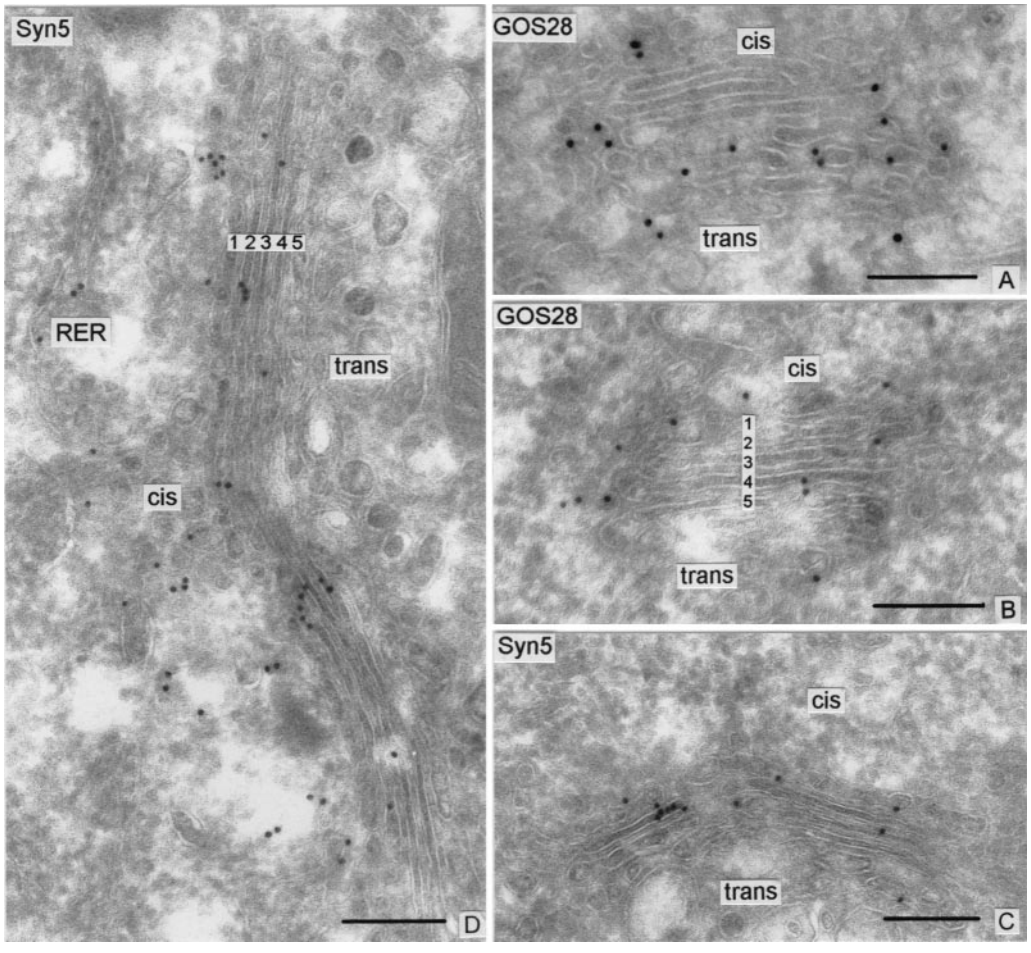

Fig. 1. Localization of GOS 28 and Syntaxin 5 in the Golgi complex of CHO or HeLa cells. Shown are representative cryosections of Golgi complexes cut in a cis–-trans orientation. The gold particles revealing GOS 28 are distributed across the stack with a preferential localization on the periphery (buds and vesicles) of the cisternae (*A* and *B*). The gold particles labeling Syntaxin 5 (Syn5) show a more central distribution on the cisternae and appear slightly more concentrated on the cis side of the stack (*C* and *D*). The five cisternae comprised in a typical stack are numbered in panels *B* and *D* (1 = cis-most; 5 = trans-most). The quantitative evaluation of the respective labeling over the Golgi cisternae and lateral vesicles is shown in Figs. 2 and 3. *A* and *B* are CHO cells; *C* and *D* are HeLa cells. RER, rough ER. (Bars represent 0.2 μm.)

stack. The cis half of the Golgi was ascribed to cisternae 1 and 2, the trans half to cisternae 3 through 5. The surface density of the labeling was evaluated by determining the area of the cisternal profiles with an electronic pen. The total cross-sectional surface area of vesicles/buds was estimated by multiplying the total number of vesicles/buds by the area of a 70-nm circle. The data are mean values obtained on 20 different Golgi areas ± SEM. Evaluation of statistical significance to test the hypothesis that GOS 28 and the KDEL receptor localize on independent populations of vesicles was done as described in ref. 23.

Results and Discussion

Cis-to-Trans Distribution of the GOS 28. GOS 28 is a SNARE protein localized to the Golgi complex (25, 27, 28), where it is efficiently packaged into COPI-coated vesicles. Fab antibodies directed at GOS 28 protein partially inhibit cell-free transport and accumulate tethered, uncoated COPI transport vesicles that fail to fuse (25). GOS 28 participates in a Golgi-restricted (28) SNARE complex with the short, Golgi-restricted spliced (29) form of Syntaxin 5 (30), suggesting the possibility that GOS 28 and the "short" form of the t-SNARE Syntaxin 5 comprise a SNARE complex (presumably with two other unidentified SNARE proteins) (5, 31) that promotes membrane fusion within the Golgi stack.

To localize the components of this SNARE complex, we used immunogold labeling of frozen sections of intact cells to localize GOS 28 and Syntaxin 5 at the electron microscope level. Anti-GOS 28 antibodies stain 33 ± 3% of the 70 to 90-nm diameter vesicles and 34 ± 7% of the buds that are on the lateral sides of transverse sections of Golgi stacks (Fig. 1 *A* and *B*, and Table 1, lines 6 and 7). From previous work, it is clear that the vast majority of the buds are COPI-coated and that the vesicles (whether still coated or subsequently uncoated) are the products of nearby buds because the vesicles do not appreciably migrate along the cis–trans axis during their lifetime (20, 23, 32).

Representative cross sections of Golgi stacks consisting of 5 cisternae were divided into cis and trans "halves," where the cis half consisted of cisternae 1 and 2, and the trans half, cisternae 3–5. The gold particles present in cisternae and in buds emanating from cisternae in each half were counted (Table 1). The trans face was positively identified in this case, and for the other antigens reported in this study, by the presence of clathrin coats which can be seen regularly in cryosections. We found that 48 ± 5% of the gold particles were present in the cis half and 52 ± 5% of the GOS 28 was present in the trans half (Table 1, lines 2 and 3). The cis–trans distribution of GOS 28 was then more precisely determined on a cisterna-by-cisterna basis (Fig. 3, triangles), establishing that GOS 28 is, within experimental technique, evenly distributed across the Golgi stack.

The same kind of analysis was performed on cryosections (Fig. 1 *C* and *D*, and Fig. 3, open circles) of cells expressing an inducible gene for the short form of Syntaxin 5. Like GOS 28, the short form of Syntaxin 5 is present throughout the stack, with the difference that the last, trans-most cisterna harbors this t-SNARE at about half the concentration of earlier cisternae. Only 9 ± 2% of the gold particles representing Syntaxin 5 were present in buds plus vesicles; the remaining 91 ± 2% were present in cisternae (Fig. 2). By contrast 42 ± 4% of the gold particles representing GOS 28 are present in lateral buds and vesicles, the remainder being in cisternal membranes (Fig. 2). This is the expected behavior for a t-SNARE subunit (Syntaxin 5) and a candidate v-SNARE (GOS 28) actively engaged in vesicle transport. Previously, Hay *et al.* (28) reported the cis–trans distribution of native Syntaxin 5 (i.e., the natural mixture of the long and short forms); their data are reproduced in Fig. 3 (filled circles). The two studies are in excellent quantitative agreement. Consistent with the earlier report of Banfield *et al.* (33), Hay *et al.* (28) report that total Syntaxin 5 is 2.3-fold more concentrated in the vesicular tubular clusters/intermediate compartment than in the Golgi stack.

In summary, both the Golgi-restricted SNARE GOS 28 and the Golgi-localized t-SNARE subunit Syntaxin 5 are present throughout the Golgi stack; Syntaxin 5 largely remains in the cisternae while GOS 28 freely enters the COPI-coated vesicles that bud from them (Figs. 1 and 2) at every level of the stack (23). These observations imply that COPI vesicles containing GOS 28 can form at every level of the stack and that the partnering t-SNARE subunit Syntaxin 5 is potentially available to fuse with these vesicles at every level of the stack.

GOS 28 Resides in the Same COPI-Coated Buds and Vesicles as Anterograde-Targeted Cargo. Two distinct populations of COPI-coated vesicles bud from Golgi cisternae at every level of the

Table 1. Distribution of GOS 28 over the Golgi complex in CHO/F3 cells

Compartment	Surface density of gold labeling, particles/μm^2	% of compartment labeled	Distribution of gold, % of total
1. Cisternae of Golgi stack	53 ± 6		49
2. Cis half	60 ± 9		48 ± 5
3. Trans half	49 ± 8		52 ± 5
4. Vesicles/buds on the cis side of the stack	70 ± 16	26 ± 5	14
5. Vesicles/buds lateral to the stack	90 ± 7	33 ± 3	37
6. Vesicles lateral to the stack	92 ± 7	33 ± 2	
7. Buds lateral to the stack	95 ± 21	34 ± 7	
8. Vesicles cis half	84 ± 15	31 ± 6	
9. Vesicles trans half	100 ± 14	34 ± 4	
10. Buds cis half	111 ± 33	33 ± 11	
11. Buds trans half	94 ± 24	36 ± 9	

CHO/F3 cells expressing myc-GOS 28. Thin sections were immunolabeled for GOS 28 with affinity-purified rabbit anti-GOS 28 (diluted 1:3), followed by goat anti-rabbit IgG gold (15-nm gold). Values are mean ± SEM from 20 different Golgi complexes.

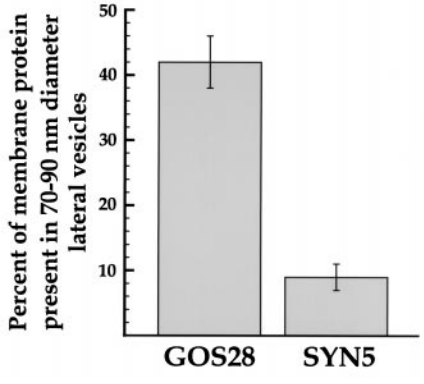

Fig. 2. Distribution of the GOS 28 and Syntaxin 5 between lateral 70- to 90-nm diameter vesicles and Golgi cisternae. The percent of gold particles present over 70- to 90-nm diameter vesicles and buds on the lateral sides of cross sections of stacks in Golgi areas was calculated as the number over such lateral buds and vesicles divided by the total of this number plus the number of gold particles over cisternae. Vesicles and buds on the cis side of the stack were excluded from this tabulation because they will include vesicular tubular clusters en route from ER to Golgi along with vesicles budding from Golgi cisternae. Bars show mean ± SEM.

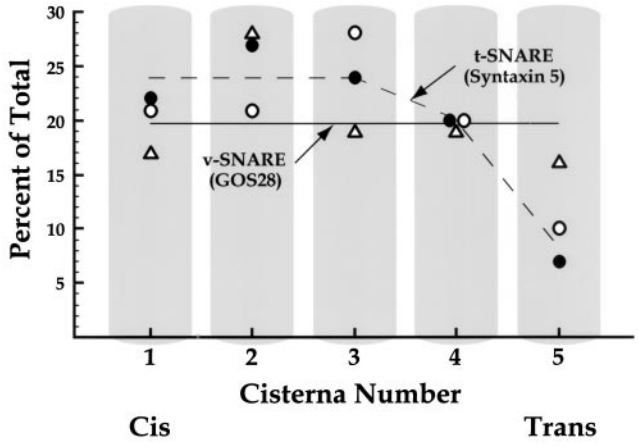

Fig. 3. Cis–trans distributions of GOS 28 (triangles) and Syntaxin 5 (open circles) across the Golgi stacks of CHO and HeLa cells, respectively. In each case, the percent of total gold particles over the Golgi stack located over a given cisterna is presented. The distribution of Syntaxin 5 in PC12 cells (closed circles) was established by Hay *et al.* (28) and is plotted according to their published data.

stack, which can be differentiated according to the nature of the cargo they carry (23). A "retrograde-selective" population contains the KDEL-signal-specific retrograde transport receptor, which functions by retrieving escaped KDEL-tagged ER resident proteins (34) and does not contain detectable anterograde-targeted cargo proteins, such as proinsulin or VSV-encoded G protein. The second, "anterograde-selective" population contains the complementary set of cargo, namely secretory and plasma membrane proteins which undergo anterograde transport, as represented by proinsulin and the VSV-encoded G protein, and lacks detectable KDEL receptor. Together, the two populations account for most and possibly all COPI-coated vesicles budding from the Golgi stack (23).

To determine whether GOS 28 is present in retrograde- or anterograde-selective transport vesicles or both, GOS 28 and the retrograde-retrieving KDEL receptor were simultaneously localized in frozen sections of intact CHO cells by using two sizes of gold particles (Fig. 4 *A* and *B*, and Table 2). Staining of vesicles and buds in both halves of stacks for both GOS 28 (Table 1) and KDEL receptor (of the gold particles located on lateral buds and vesicles, 62 ± 10% were in the cis half and 38 ± 10% were in the trans half of the stack; not shown) were clearly evident, yet no colocalization of these two proteins was found (Table 2). This was true both for vesicles on the cis side and for vesicles lateral to cross sections of Golgi stacks. For example, in the lateral vesicle population, while 25 ± 3% labeled for KDEL receptor and 22 ± 3% labeled for GOS 28, only a trace level, 2 ± 1%, labeled for both. Given the frequencies for single labeling, the hypothesis that the two proteins are distributed in a single population of vesicles can be rejected at the $P < 0.025$ level (cis vesicles) and $P < 0.004$ (lateral vesicles) level of statistical significance.

Therefore, GOS 28 is either absent or below the limits of detection in the retrograde population of vesicles. It logically follows that GOS 28 is selectively contained in the other population of Golgi-derived COPI vesicles (i.e., anterograde-selective vesicles). To confirm this conclusion, GOS 28 and VSV G protein were colocalized in VSV-infected CHO cells (Fig. 4 *C* and Table 3). A total of 44 ± 4% of the anterograde-selective population of lateral buds and vesicles, marked by VSV G protein, also contained GOS 28. This is, of course, a minimum

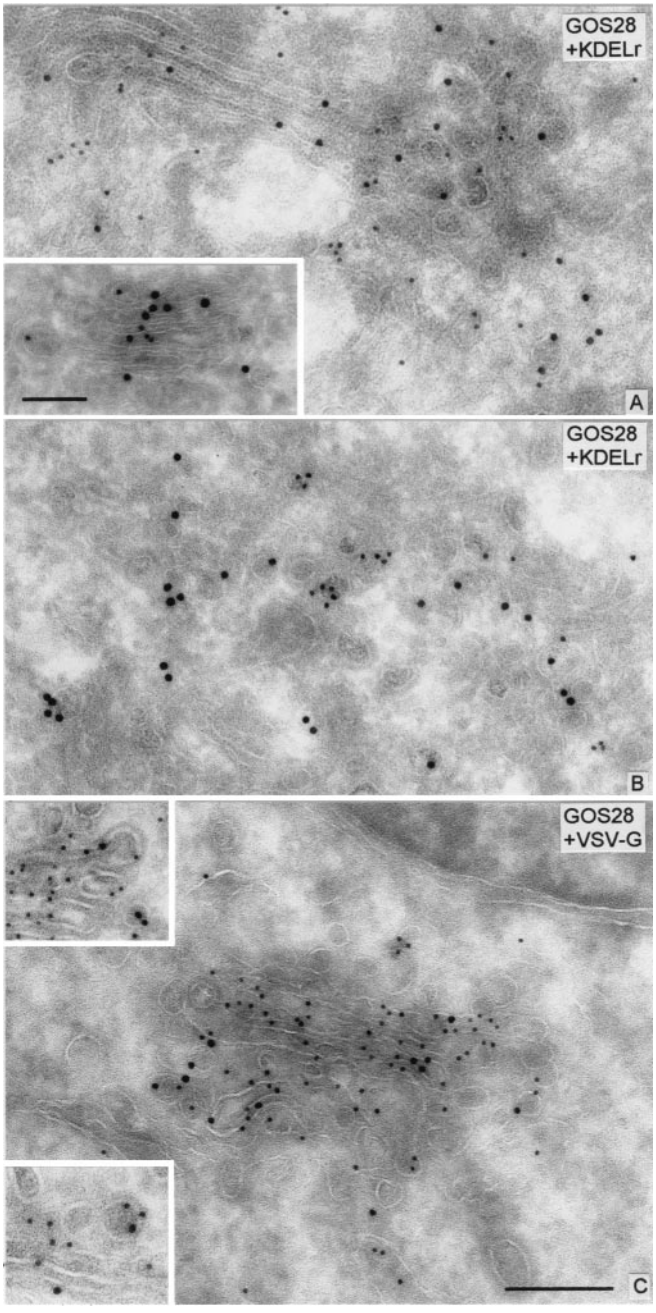

Fig. 4. Double immunolabeling of GOS 28 and KDEL receptor (KDELr), or GOS 28 and VSV-G in the Golgi complex of CHO cells. The small gold particles revealing GOS 28 show no colocalization with large gold particles revealing KDELr on the cisternal buds and vesicles (*A* and *B*). Colocalization of GOS 28 and KDELr is detectable only on the stacked cisternae (*A* and *Inset* in *A*). The large gold particles revealing GOS 28 colocalize with the small gold particles labeling VSV-G protein on cisternae, coated buds (upper *Inset* in *C*), or vesicles (lower *Inset* in *C*). The quantitative evaluation of the labeling is shown in Table 2. [The bar shown in *C* (0.2 μm) applies for the upper *Inset* in *C* and for *A* and *B*. The bar shown in the *Inset* in *A* (0.1 μm) applies for the lower *Inset* in *C*.]

figure because of the relative inefficiency of antigen staining characteristic of double-label experiments.

The density of labeling for GOS 28 in the total population of lateral vesicles is 92 ± 7 gold particles per μm^2 (Table 1, line 6). Considering only those vesicles lateral to the stack that have one or more gold particles (i.e., 33 ± 3% of the total) which are now seen to be anterograde-selective, these vesicles have a gold

Table 2. Simultaneous localization of KDEL receptor and GOS 28 over the Golgi complex in CHO/F3 cells

70- to 90-nm diameter vesicle labeling	% vesicles located	
	On cis side of stack	On lateral side of stack
KDEL receptor only	28 ± 5	25 ± 3
myc-GOS 28 only	16 ± 3	22 ± 3
Both proteins	0	2 ± 1

CHO/F3 cells expressing myc-GOS 28. Thin sections were double-labeled for KDEL receptor and GOS 28 with rabbit polyclonal anti-KDEL receptor and mouse monoclonal anti-myc 9E10 antibodies, followed by goat anti-rabbit IgG gold (15-nm gold) and goat anti-mouse IgG gold (10-nm gold). The quantitative evaluation was performed on 20 separate Golgi areas. Data are mean ± SEM.

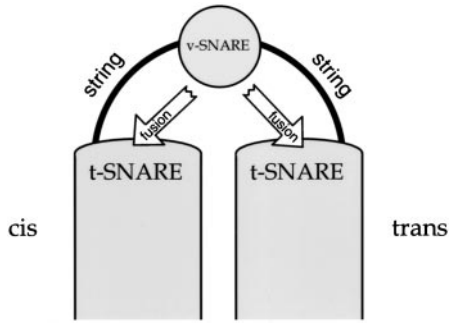

Fig. 5. Anterograde transport mediated by bidirectionally moving COPI vesicles. See text for details of this model.

density of 275 ± 7 particles per μm^2 (not shown). When compared with the density of labeling for GOS 28 of 53 ± 6 particles per μm^2 (Table 1, line 1) in the Golgi cisternae, it can be concluded that GOS 28 is enriched in vesicles by an upper limit of 275/53 = 5.2-fold during the budding of anterograde-selective COPI vesicles from Golgi cisternae *in vivo* and is excluded from retrograde-selective vesicles.

Anterograde Flow Potentially Mediated by "Percolating" COPI Vesicles. GOS 28 resides in the COPI vesicles bearing anterograde-targeted cargo. Because this SNARE and its partnering t-SNARE heavy chain are present throughout the stack, the potential clearly exists for a vesicular pathway that can carry exported proteins all of the way from the cis to the trans face. In the absence of any further constraints, a GOS 28-containing vesicle budding at any level of the stack could potentially fuse via SNARE complexes containing both GOS 28 and syntaxin 5 with any cisterna at any level. It is presently unclear whether GOS 28 functions as a v-SNARE or as a light chain of a t-SNARE (5) or both.

However, COPI vesicles at every level are tethered to cisternae throughout the stack by flexible "strings"—tethers that are long enough to permit vesicles to reach the adjoining cisternae on either side—effectively restraining transfers to the nearest neighbors in the stack (32, 35). One system of strings, located at the cis face of the stack, has been well-characterized. It consists of end-to-end complexes of giantin, p115, GM130, GRASP-65, and even tether COPI vesicles as they bud (35–41).

Because of tethering, COPI vesicles are restricted (32, 35) to delivering their quanta of cargo to the neighboring cisternae on the cis or trans side, this choice potentially being made on a stochastic (probabilistic) basis in light of our findings (Fig. 5). The simplest stochastic process is a bidirectional random walk up and down the stack by "percolating" GOS 28 COPI vesicles, which would serve to equilibrate exported proteins among the cisternae, preventing a cis–-trans concentration gradient of anterograde cargo from forming. Recycling of SNAREs (GOS 28) and other machinery of anterograde-selective vesicles and balancing of membrane flow would occur as an automatic consequence of the bidirectionality. Because successive cisternae would be first encountered in sequence, processing enzymes will be encountered in sequential order, and distillation will still occur (22).

Table 3. Simultaneous localization of VSV G protein and GOS 28 in CHO/F3 cells

70- to 90-nm diameter vesicles and buds on the lateral side of stack labeling	% of vesicles/buds labeled	% of VSV G-positive vesicles/buds also staining for GOS 28
VSV G only	18 ± 2	—
GOS 28 only	21 ± 2	—
Both proteins	11 ± 1	44 ± 4

CHO/F3 cells were infected with VSV for 1 h then incubated with VSV-free medium for 2 h before fixation. Thin sections were double-labeled with mouse monoclonal anti-VSV G protein antibodies (P5D4) and affinity-purified rabbit anti-GOS 28 (diluted 1:5), followed by goat anti-mouse IgG gold (10-nm gold) and goat anti-rabbit IgG gold (15-nm gold). The quantitative evaluation was performed on 40 Golgi areas at a magnification of ×72,000. Data are mean ± SEM.

While individual quanta of cargo move in either direction at every level of the stack, a net flow of exported protein in the cis-to-trans direction would nonetheless result because entry and exit of cargo occur at opposite ends of this stack. This is analogous to what happens when water flows through a pipe: water enters only at one end and exits only at the other and therefore flows through; yet individual water molecules (like the quanta of cargo in the Golgi stack) diffuse either with and against the flow with equal probability. Polarized delivery of cargo to the cis end of the stack likely results from the capture of ER-derived vesicles before SNARE complex assembly by the p115-containing tethers that emanate exclusively from the cis face (36–38, 42). Polarized exit from the trans face (trans-Golgi network) is well established (43).

The net rate of flow of anterograde cargo in the cis-to-trans direction could be enhanced above a truly random walk by additional asymmetries that could systematically bias the probability of fusion of GOS 28-piloted COPI vesicles toward the trans rather than toward the cis face of the stack, including potential subspecies of Syntaxin 5-containing intra-Golgi t-SNAREs (28, 44) and different tethering systems that could potentially be asymmetrically distributed along the cis–-trans axis. However, even a completely random walk can be surprisingly efficient: it has been estimated that an average of only 9–10 vesicle transfers are required for cargo to transit a stack of 5 cisternae (see figure 2 at $r = 1$ in ref. 14).

Whatever the detailed mechanism, the possibility that COPI vesicles containing cargo that will ultimately exit at the trans face of the Golgi stack can move bidirectionally is now an attractive model. Therefore, we now prefer to use the term "anterograde cargo-*selective* " rather than the former term "anterograde-*directed*"(23) to describe this population of COPI vesicles. This is not to imply that the anterograde cargo-selective COPI vesicles necessarily achieve their specific content by direct receptor binding of anterograde cargo; it could well be that retrograde, KDEL receptor COPI vesicles are intrinsically selective and that the percolating GOS 28-COPI vesicles are bulk carriers (45, 46). Either way, the overall effect is that the GOS 28-COPI vesicles are functionally selective for anterograde-targeted proteins.

The model also implies that forward and backward movement in the stack result from the same underlying process. This would reconcile seemingly discordant observations about

Golgi transport in a straightforward fashion. Entry of glycosyltransferases and other resident proteins into percolating COPI vesicles would allow cis–trans gradients of these Golgi constituents to be maintained as a result of dynamic equilibria (22, 47), even though these resident proteins enter vesicles at low concentrations (17, 48). Percolating COPI vesicles (Fig. 5) containing even low levels of glycosyltransferases, along with anterograde-targeted cargo, would also explain why cell-free incubations of Golgi membranes result both in transfer of VSV G protein from glycosyltransferase-free ''donor'' stacks to glycosyltransferase-containing ''acceptor'' stacks (19–21, 49), and in transfer of catalytically active glycosyltransferase from ''acceptor'' stacks to ''donor'' stacks (50). In the hindsight of two decades, the cell-free Golgi transport assay (49) can be seen to reconstitute a spectrum of activities of COPI-coated vesicles, reflecting a then-unanticipated richness of their role in establishing the pattern of macromolecular flow within the Golgi stack.

This work was supported by a Swiss National Science Foundation grant (to L.O.), and a National Institutes of Health grant (to J.E.R.), and by postdoctoral fellowships from the Medical Research Council of Canada (to A.V.), Deutsche Forschungsgemeinschaft (to T.E.), and the Max Kade Foundation (to M.G).

1. Söllner, T., Whiteheart, S. W., Brunner, M., Erdjument-Bromage, H., Geromanos, S., Tempst, P. & Rothman, J. E. (1993) *Nature (London)* **362,** 318–324.
2. Weber, T., Zemelman, B. V., McNew, J. A., Westermann, B., Gmachl, M., Parlati, F., Söllner, T. H. & Rothman, J. E. (1998) *Cell* **92,** 759–772.
3. McNew, J. A., Parlati, F., Fukuda, R., Johnston, R. J., Paz, K., Paumet, F., Söllner, T. H. & Rothman, J. E. (2000) *Nature (London)*, in press.
4. Parlati, F., McNew, J. A., Fukuda, R., Miller, R., Söllner, T. H. & Rothman, J. E. (2000) *Nature (London)*, in press.
5. Fukuda, R., McNew, J. A., Weber, T., Parlati, F., Engel, T., Nickel, W., Rothman, J. E. & Söllner, T. H. (2000) *Nature (London)*, in press.
6. Rothman, J. E. (1994) *Nature (London)* **372,** 55–63.
7. Pfeffer, S. (1999) *Nat. Cell Biol.* **1,** E17–E22.
8. Waters, M. G. & Pfeffer, S. R. (1999) *Curr. Opin. Cell Biol.* **11,** 453–459.
9. Guo, W., Sacher, M., Barrowman, J., Ferro-Novick, S. & Novick, P. (2000) *Trends Cell Biol.* **10,** 251–255.
10. Nichols, B. J. & Pelham, H. R. (1998) *Biochim. Biophys. Acta* **1404,** 9–31.
11. Hardwick, K. G. & Pelham, H. R. (1992) *J. Cell Biol.* **119,** 513–521.
12. Holthuis, J. C., Nichols, B. J., Dhruvakumar, S. & Pelham, H. R. (1998) *EMBO J.* **17,** 113–126.
13. Pelham, H. R. (1998) *Trends Cell Biol.* **8,** 45–49.
14. Glick, B. S., Elston, T. & Oster, G. (1997) *FEBS Lett.* **414,** 177–181.
15. Bonfanti, L., Mironov, A. A., Jr., Martinez-Menarguez, J. A., Martella, O., Fusella, A., Baldassarre, M., Buccione, R., Geuze, H. J., Mironov, A. A. & Luini, A. (1998) *Cell* **95,** 993–1003.
16. Bonfanti, L., Martella, O., Mironov, A. & Luini, A. (1999) *Mol. Biol. Cell* **10,** Suppl., 114a.
17. Orci, L., Amherdt, M., Ravazzola, M., Perrelet, A. & Rothman, J. E. (2000) *J. Cell Biol.*, in press.
18. Volchuk, A., Amherdt, M., Ravazzola, M., Rivera, V. M., Clackson, T., Perrelet, A., Söllner, T. H., Rothman, J. E. & Orci, L. (2000) *Cell* **102,** 335–348.
19. Orci, L., Glick, B. S. & Rothman, J. E. (1986) *Cell* **46,** 171–184.
20. Orci, L., Malhotra, V., Amherdt, M., Serafini, T. & Rothman, J. E. (1989) *Cell* **56,** 357–368.
21. Ostermann, J., Orci, L., Tani, K., Amherdt, M., Ravazzola, M., Elazar, Z. & Rothman, J. E. (1993) *Cell* **75,** 1015–1025.
22. Rothman, J. E. & Wieland, F. T. (1996) *Science* **272,** 227–234.
23. Orci, L., Stamnes, M., Ravazzola, M., Amherdt, M., Perrelet, A., Söllner, T. H. & Rothman, J. E. (1997) *Cell* **90,** 335–349.
24. Letourneur, F., Gaynor, E. C., Hennecke, S., Demolliere, C., Duden, R., Emr, S. D., Riezman, H. & Cosson, P. (1994) *Cell* **79,** 1199–1207.
25. Nagahama, M., Orci, L., Ravazzola, M., Amherdt, M., Lacomis, L., Tempst, P., Rothman, J. E. & Söllner, T. H. (1996) *J. Cell Biol.* **133,** 507–516.
26. Griffiths, G., Ericsson, M., Krijnse, L. J., Nilsson, T., Goud, B., Soeling, H. D., Tang, B. L., Wong, S. H. & Hong, W. (1994) *J. Cell Biol.* **127,** 1557–1574.
27. Subramaniam, V. N., Peter, F., Philp, R., Wong, S. H. & Hong, W. (1996) *Science* **272,** 1161–1163.
28. Hay, J. C., Klumperman, J., Oorschot, V., Steegmaier, M., Kuo, C. S. & Scheller, R. H. (1998) *J. Cell Biol.* **141,** 1489–1502.
29. Hui, N., Nakamura, N., Sönnichsen, B., Shima, D. T., Nilsson, T. & Warren, G. (1997) *Mol. Biol. Cell* **8,** 1777–1787.
30. Bennett, M. K., Garcia-Arraras, J. E., Elferink, L. A., Peterson, K., Fleming, A. M., Hazuka, C. D. & Scheller, R. H. (1993) *Cell* **74,** 863–873.
31. Sutton, R. B., Fasshauer, D., Jahn, R. & Brunger, A. T. (1998) *Nature (London)* **395,** 347–353.
32. Orci, L., Perrelet, A. & Rothman, J. E. (1998) *Proc. Natl. Acad. Sci. USA* **95,** 2279–2283.
33. Banfield, D. K., Lewis, M. J., Rabouille, C., Warren, G. & Pelham, H. (1994) *J. Cell Biol.* **127,** 357–371.
34. Pelham, H. R. B. (1996) *Cell Struct. Funct.* **21,** 413–419.
35. Sönnichsen, B., Lowe, M., Levine, T., Jamsa, E., Dirac-Svejstrup, B. & Warren, G. (1998) *J. Cell Biol.* **140,** 1013–1021.
36. Sapperstein, S. K., Lupashin, V. V., Schmitt, H. D. & Waters, M. G. (1996) *J. Cell Biol.* **132,** 755–767.
37. Barlowe, C. (1997) *J. Cell Biol.* **139,** 1097–1108.
38. Nelson, D. S., Alvarez, C., Gao, Y. S., Garcia-Mata, R., Fialkowski, E. & Sztul, E. (1998) *J. Cell Biol.* **143,** 319–331.
39. Shorter, J. & Warren, G. (1999) *J. Cell Biol.* **146,** 57–70.
40. Nakamura, N., Rabouille, C., Watson, R., Nilsson, T., Hui, N., Slusarewicz, P., Kreis, T. E. & Warren, G. (1995) *J. Cell Biol.* **131,** 1715–1726.
41. Barr, F. A., Puype, M., Vandekerckhove, J. & Warren, G. (1997) *Cell* **91,** 253–262.
42. Nakamura, N., Lowe, M., Levine, T. P., Rabouille, C. & Warren, G. (1997) *Cell* **89,** 445–455.
43. Griffiths, G. & Simons, K. (1986) *Science* **234,** 438–443.
44. Hay, J. C., Chao, D. S., Kuo, C. S. & Scheller, R. H. (1997) *Cell* **89,** 149–158.
45. Karrenbauer, A., Jeckel, D., Just, W., Birk, R., Schmidt, R. R., Rothman, J. E. & Wieland, F. T. (1990) *Cell* **63,** 259–267.
46. Warren, G. & Mellman, I. (1999) *Cell* **98,** 125–127.
47. Bretscher, M. S. & Munro, S. (1993) *Science* **261,** 1280–1281.
48. Sönnichsen, B., Watson, R., Clausen, H., Misteli, T. & Warren, G. (1996) *J. Cell Biol.* **134,** 1411–1425.
49. Balch, W. E., Dunphy, W. G., Braell, W. A. & Rothman, J. E. (1984) *Cell* **39,** 405–416.
50. Love, H. D., Lin, C. C., Short, C. S. & Ostermann, J. (1998) *J. Cell Biol.* **140,** 541–551.